

Peak directivity analysis of far-field acoustical measurements during three GEM 63 static firings

Michael S. Bassett, Kent L. Gee, Grant W. Hart, et al.

Citation: *Proc. Mtgs. Acoust.* **39**, 040004 (2019); doi: 10.1121/2.0001467

View online: <https://doi.org/10.1121/2.0001467>

View Table of Contents: <https://asa.scitation.org/toc/pma/39/1>

Published by the [Acoustical Society of America](#)

ARTICLES YOU MAY BE INTERESTED IN

[Characterization of Falcon 9 launch vehicle noise from far-field measurements](#)

The Journal of the Acoustical Society of America **150**, 620 (2021); <https://doi.org/10.1121/10.0005658>

[Experimental study on effects of plate angle on acoustic waves from supersonic impinging jets](#)

The Journal of the Acoustical Society of America **150**, 1856 (2021); <https://doi.org/10.1121/10.0006236>

[Summary of Acoustics-in-Focus Panel Discussion Special Session "Underwater Sound Modeling: Comprehensive Environmental Descriptions"](#)

Proceedings of Meetings on Acoustics **43**, 002001 (2021); <https://doi.org/10.1121/2.0001469>

[Using a kilometers-long horizontal multichannel array for estimating seafloor sound speed in a passive margin setting](#)

Proceedings of Meetings on Acoustics **44**, 005002 (2021); <https://doi.org/10.1121/2.0001466>

[Influence of the supporting table on initial transients of the fretted zither: An impulse pattern formulation model](#)

Proceedings of Meetings on Acoustics **43**, 035003 (2021); <https://doi.org/10.1121/2.0001494>

[Development of formant frequency distributions in American English-speaking elementary school-aged children: A longitudinal study](#)

Proceedings of Meetings on Acoustics **42**, 060016 (2020); <https://doi.org/10.1121/2.0001459>



What makes a good POMA article?

[LEARN MORE](#)

178th Meeting of the Acoustical Society of America

San Diego, California

2-6 December 2019

Noise: Paper 4pNS6**Peak directivity analysis of far-field acoustical measurements during three GEM 63 static firings****Michael S. Bassett, Kent L. Gee, Grant W. Hart, Logan T. Mathews, Reese D. Rasband and Daniel J. Novakovich***Department of Physics and Astronomy, Brigham Young University, Provo, UT, 84602;
MichaelScottBassett@physics.byu.edu; kentgee@byu.edu; grant_hart@byu.edu;
loganmathews103@gmail.com; r.rasband18@gmail.com; danielnovakovich@gmail.com*

This study investigates far-field rocket noise from three static firings of the Northrop Grumman GEM 63 motor. In addition to determining the peak directivity angle from measurements, this paper considers the overall sound pressure level, spectra, and skewness of the pressure time derivative. Although there is temporal variability in overall level during each firing, linked to variation in thrust and possibly wind, the peak directivity during the maximum thrust period is located around 62-63° for all three firings. Additionally, the analysis shows that nonlinear acoustic propagation effects remain significant around the peak directivity direction at distances around 1.5 km. Overall levels, spectral high-frequency content, and derivative skewness are greater at larger angles when there is wind with an upstream component.

1. INTRODUCTION

With the renewed interest in space exploration from governments and private businesses, the number of launch vehicles, launch pads, and the frequency of launches around the world will continue to increase, and potential impacts should be studied. The current understanding of the fundamental physics of rocket exhaust plumes is somewhat limited and still based in part on Apollo Program-era understandings^{1,2} with relatively few studies returning new experimental data from full-scale rocket measurements and vehicle launches. The rocket noise literature shows some historical discrepancies in peak directivity angles being somewhere between 50-75° relative to the plume.²⁻⁵ In NASA SP 8072 the peak radiation from a “standard chemical rocket” was described as 50-55° from the direction of the plume.¹ The National Aeronautics and Space Administration (NASA) made measurements to update the peak directivity for the reusable solid rocket motor (RSRM) as part of the Ares program⁶⁻⁷ and also found the peak radiation angle to be around 55°, but it was ultimately determined that the measurement arc was not taken in the far field. The measurements also did not account for the main source location being about 18 nozzle diameters (18D) downstream of the nozzle.⁸ James *et al.*⁹ reanalyzed the measurements by adjusting the angles to account for a frequency-dependent source location. With the adjusted angles the peak directivity was predicted to be around 64°, which fits the angle predicted by the convective Mach number of the plume.⁹ However, the literature appears to lack a far-field measurement that clearly shows this peak directivity angle of ~65° for a large solid fuel booster. The primary purpose of this paper is to show that, in the far field, the peak directivity angle for overall sound pressure level (OASPL) radiated from a large solid-fuel rocket motor is in the vicinity of 65°. Additionally, the analysis shows that nonlinear acoustic propagation effects remain significant around the peak directivity direction.

Brigham Young University (BYU) has previously made other noise measurements of static motor tests held at Northrop Grumman Innovative Systems’ (NGIS) facility located in northern Utah, near Promontory, UT.¹⁰⁻¹³ Some of these tests focused on near-field source localization and others on far-field characteristics. However, although near-field vector intensity measurements¹¹ indicated a directivity angle greater than 60° for most of the frequency range, none of these measurements contained a sufficient number of far-field microphones to experimentally confirm the far-field peak directivity. These measurements of the Northrop Grumman GEM 63 motor, compiled from three separate firings, help accomplish this purpose and allow for some comparison across tests. This paper discusses the measurement setups, as well as other important features relevant for data analysis, such as the local meteorology and surrounding terrain.

2. DATA COLLECTION SETUPS

The GEM 63 solid-fuel booster (shown in Figure 1) has a casing diameter of 1.6 m (63.2”), a length of 20.1 m (792.2”), and a nozzle exit diameter of 1.49 m (58.8”). Designed for the Atlas V launch vehicle, the motor provides a maximum of 1.65 MN (370,835 lbf) of thrust and burns for 97.6 seconds under nominal conditions in a vacuum.¹⁴ Figure 2 shows the GEM 63 firing in the T-6 test bay, as observed from one of the measurement sites. The first of the recorded firings occurred in September of 2018 and the second and third recorded firings took place in April and October of 2019, respectively.



Figure 1. Picture of GEM 63 motor from NGIS catalog.¹⁴



Figure 2. Firing of the GEM 63 motor at the NGIS facility.

Acoustic pressure waveform measurements were taken at an average distance of approximately 1 mile (1.6 km) from the rocket motor (see Tables 1-3) along a two-lane highway outside of the NGIS facility. Instead of relying on long cable runs from a central station, each station was run by one of BYU's Portable Units for Measuring Acoustics (PUMA).¹⁵ The data were recorded onto a Surface Pro that controlled a National Instruments data acquisition (DAQ) system, as shown in Figure 3. Depending on the capabilities of the DAQ module, the sampling frequencies were 50 kHz, 51.2 kHz or 102.4 kHz. Each station was time-synchronized using an IRIG-B GPS Clock to allow for future correlation analyses. Small meteorological units were included at a few stations for recording meteorological data such as temperature, humidity, wind speed and direction, and atmospheric pressure. The general measurement setup was the same for each of the three recordings, with some variation in station placement to focus on different areas. Regardless of the variations, the microphones used in this analysis were 1/2" type 1 free-field or pressure microphones from GRAS Sound and Acoustics or PCB Piezotronics with comparable acoustical responses.



Figure 3. Example of a PUMA setup.

One of the main objectives of the measurement in September was to confirm the shape/location of the main radiation lobe of the sound propagated into the far field. This was accomplished using eleven different measurement stations, spanning from 40° to 110° from the plume direction (red line) as shown in Figure 4. Terrain shielding prevented stations at and upstream of 80° from having complete line of sight to the motor. The red line shows the direction of the exhaust plume and represents 0° . Based on the results from September, the April recording aimed to focus on an area spanning a smaller region of 50 - 83° to get a better resolution of the peak angle of the main radiation lobe (See Figure 5). The October recording stayed within the smaller span of angles but shifted slightly to cover 45 - 75° (See Figure 6).

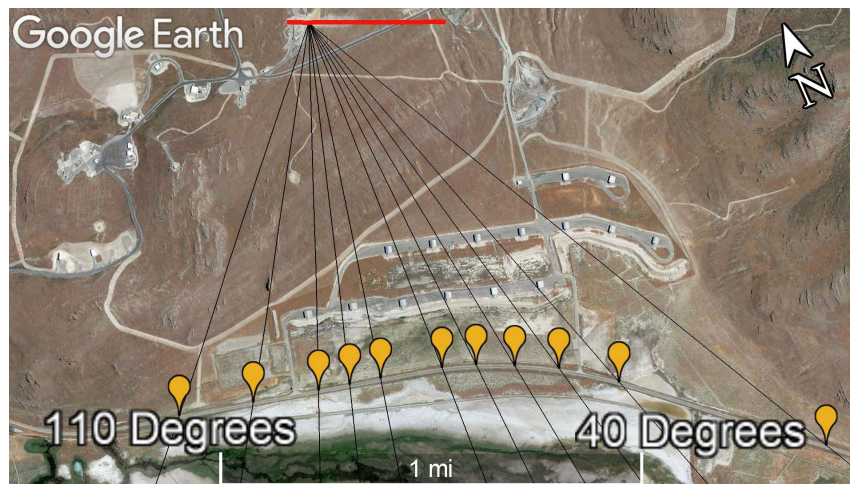


Figure 4. Layout of the measurement setup for September 2018 as shown on Google Earth.

Table 1. Distances from the rocket nozzle to the measurement stations in September 2018. Shaded columns indicate stations that had limited (light) or no (dark) line of sight to the motor from the recording station.

Distance (km)	1.56	1.44	1.37	1.36	1.35	1.38	1.42	1.49	1.59	1.79	2.51
Angle (degrees)	110	100	90	85	80	70	65	60	55	50	40

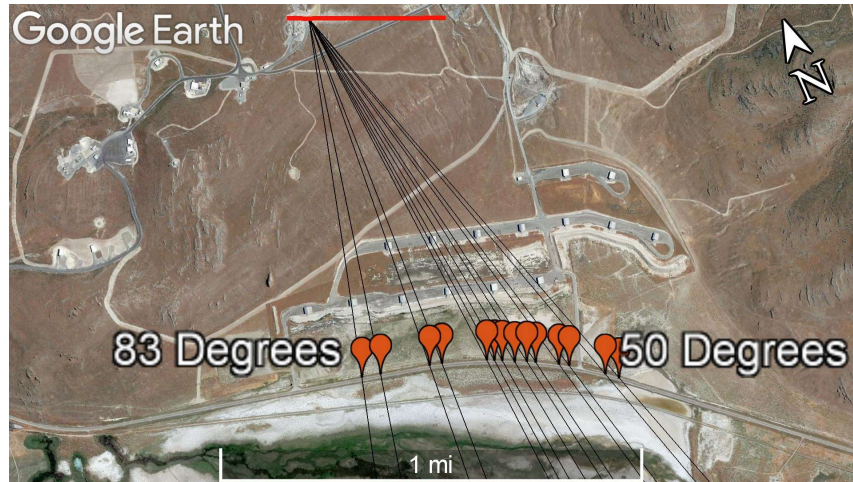


Figure 5. Layout of the measurement setup for April 2019 as shown on Google Earth.

Table 2. Distances from the rocket nozzle to the measurement stations in April 2019. Shaded columns indicate stations that had limited line of sight.

Distance (km)	1.35	1.35	1.37	1.38	1.44	1.45	1.47	1.49	1.52	1.54	1.59	1.62	1.73	1.78
Angle (degrees)	83	80	72	70	63.5	62.5	61.5	60	58.5	57.5	55	54	51	50

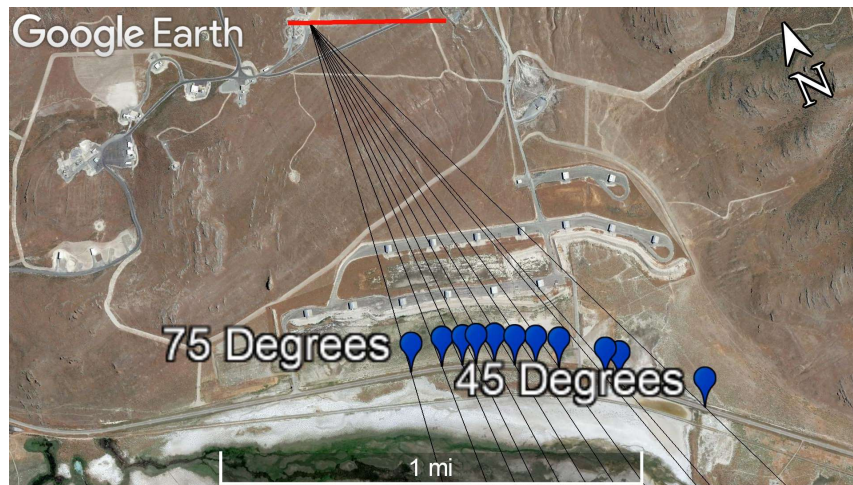


Figure 6. Layout of the measurement setup for October 2019 as shown on Google Earth.

Table 3. Distances from the rocket nozzle to the measurement stations in October 2019.

Distance (km)	1.36	1.38	1.4	1.42	1.45	1.49	1.54	1.59	1.73	1.78	2.05
Angle (degrees)	75	70	67	65	62.5	60	57.5	55	51	50	45

3. RESULTS/DATA ANALYSIS

A. WAVEFORMS

Comparing the OASPL and pressure from the different stations as shown in Figure 7, we see some variations in the profiles. Some of these changes are caused because the measurement stations are located across different sections of the main radiation lobe. Other changes are due to the terrain effects around the test site. Figure 2 shows that the site of the testing bay is elevated from the measurement sites, and that the ground is rough with elevation changes between the recording site and test bay. Despite these differences, the profiles all have the same general shape, which matches well against the thrust profile of the motor, as seen in Figure 8. The first section ramps up for the initial firing and stays there for about 30 seconds, after which it dies down before slightly ramping back up for after the launch vehicle passes through maximum dynamic pressure. Analyzing smaller sections of time helped to focus on areas where the profile was mostly consistent. To define these smaller sections, the OASPL was calculated for each file. Then 20 seconds of data (represented by the section contained between the vertical green lines in Figure 7) were taken starting 10 seconds past the first instance that the SPL came within 6 dB of the maximum OASPL.

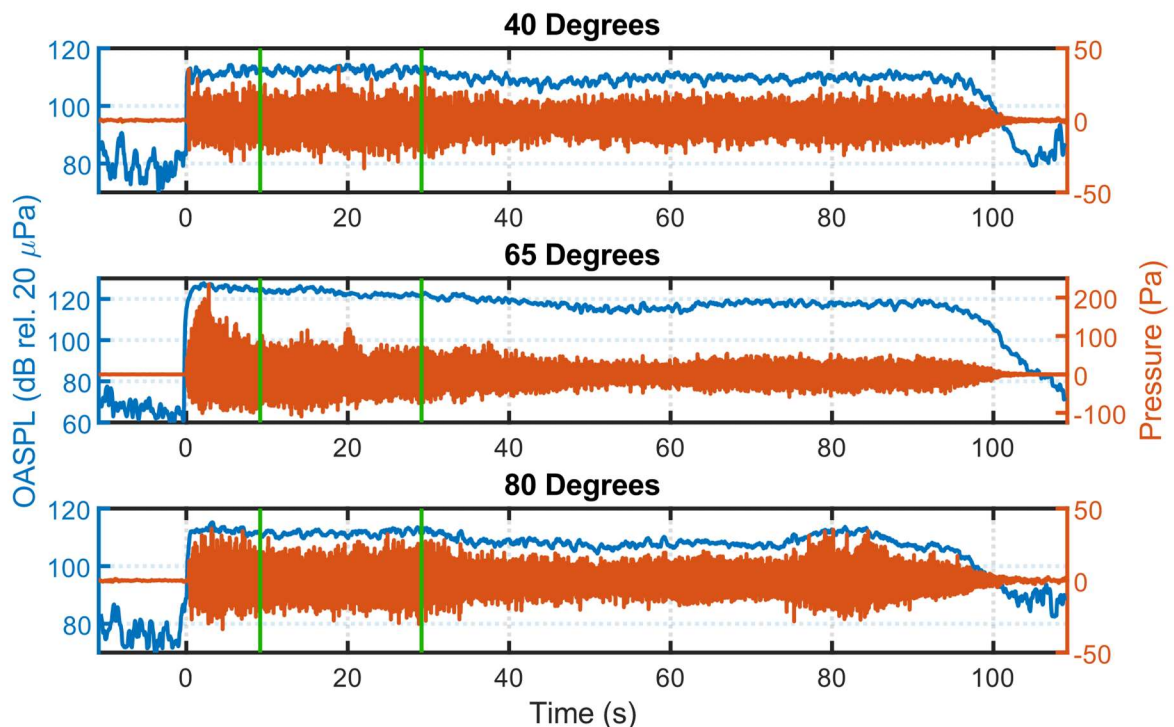


Figure 7. Time waveforms from three separate stations during the September firing. The vertical green lines show the 20 second section that was used for analysis.

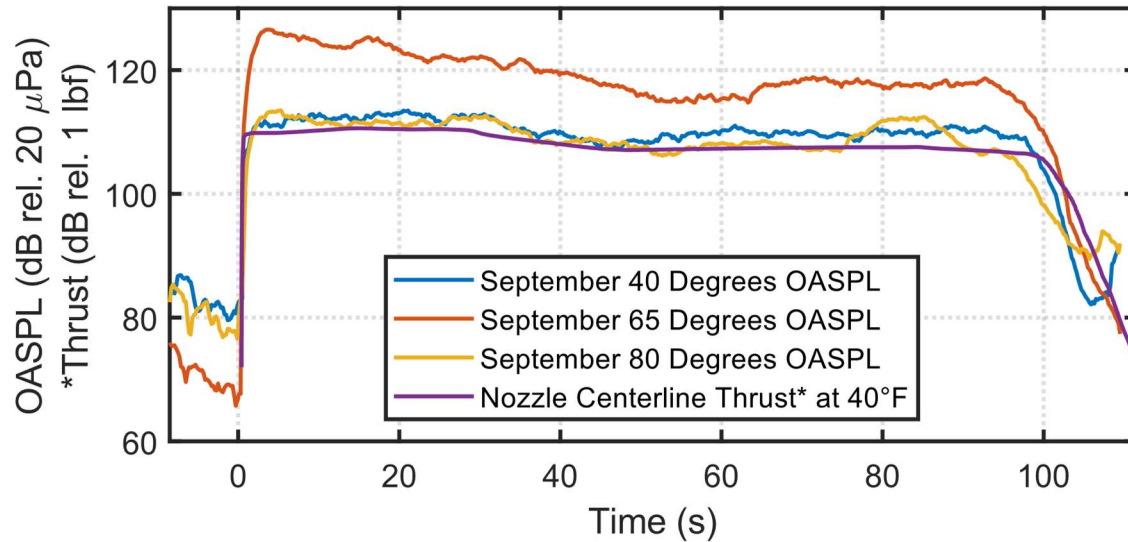


Figure 8. OASPL from three September stations compared to the nominal Nozzle Centerline Thrust for the motor being cooled to 40 °F.

B. DIRECTIVITY

Plotting the distance-corrected OASPL from the first channel of each station across the three recordings, as shown in Figure 9, a peak can be seen around 60° to 65°, particularly for the September recording. Because the stations were at difference distances from the sound source, spherical spreading corrections were used to calculate the OASPL at a distance of 100D. This correction seems to have over-estimated the levels at 40° to 45° because they were significantly farther from the source than the other stations. Stations between 80° to 110° have limited or no line-of-sight to the motor during the firing so their levels drop faster than what is expected from the literature. A quadratic curve fitting of the OASPL versus angle, with available points between 50° and 80° from each recording, found all three peaks to be between 62° and 63°. This agrees with predictions based on calculations involving the angle of the nozzle plume and the convective Mach number.⁹ (The convective Mach number for the GEM 63 is assumed to be similar to that of the RSRM.) As previously mentioned, the measurement setup from April aimed to focus on angles where the OASPL peaks. The expected result for April would have been to get a higher resolution of a main radiation lobe that maintained the same general shape, level, and relative position as measured in September. The actual results show that the shape widened, the highest peak lowered, and levels increased at angles further from the plume direction. October also had a widened range, though it seems to have done so more evenly to both sides compared to September.

Regarding OASPL at 100D, the levels appear to be 143-144 dB. These levels approximately agree with the RSRM predictions by James *et al.*⁹ suggesting the similarity between these motors. Additionally, these distance-scaled levels can be compared with those predicted using a graphical curve by Greska *et al.* for different convective Mach numbers. Given the Oertel convective Mach number of approximately 2.3,⁹ Greska *et al.*¹⁶ predicts a maximum OASPL at 100D along the peak directivity angle of 144 dB. Mathews *et al.*^{17,18} showed a datapoint representing the predicted⁹ RSRM levels of 143 dB and further compared the Greska *et al.* model to Falcon 9 launch data. These measurements represent an additional point of comparison for the Greska *et al.* model for these high convective Mach number jets.

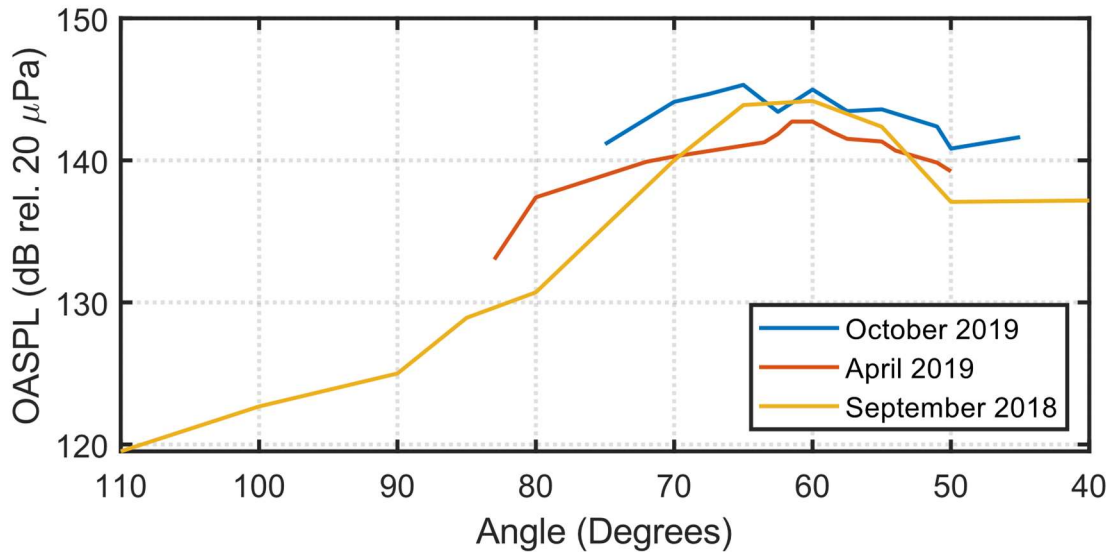


Figure 9. Comparison in directivity between firings using the OASPL, distance-corrected to 100D, from the first channel of every station.

C. WIND DIRECTION/TEMPORAL DIFFERENCES

Because all measurements were made with the same rocket motor and the test setups between the three firings were not significantly different, the question arises if there were any measured conditions during each test that could explain the differences in the shape of the directivity lobe. Looking at the weather data, April had somewhat strong wind (4.4 m/s) that blew upstream, relative to the plume direction, while September's wind was less than half of that (1.8 m/s) and blew more downstream. It seems reasonable that this change in wind may provide an explanation for the change in directivity lobe shape. Namely, the wind in April altered the sound directivity, causing the slight drop at 60-65° and the increase in OASPL at stations farther upstream.

D. SPECTRA

The comparison of spectra in Figure 10 shows differences between firings for three different stations. The spectra for each measurement at 50° are consistent across most frequencies. At the 60° and 70° stations, there is a more noticeable difference in the spectra. Up to 100-200 Hz, the spectra follow a similar trend. At higher frequencies, the levels are noticeably higher in September at 60° but then at 70° higher levels in this frequency band occur in April. This shift correlates with the wind during April.

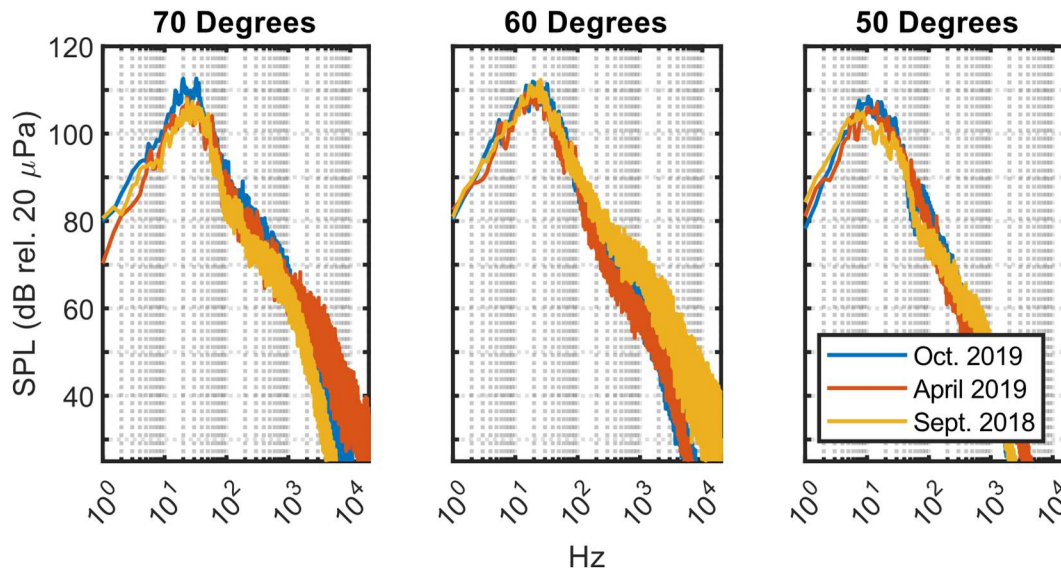


Figure 10. Comparing the spectra between similar stations across the firings.

E. DERIVATIVE SKEWNESS

Derivative skewness (dSk) is a measure for shock content and the perception of the psychoacoustic phenomenon known as crackle. Increased dSk values correlate to greater energy at higher frequencies, so the shift in higher frequencies could be caused by a shift in the directivity of dSk. A dSk value above 3 is perceived as having crackle, with values above 9 containing persistent and intense crackle.¹⁹ As shown in Figure 11, the dSk peaks for all these firings are far above the threshold for intense crackle. Because the shocks that contribute to dSk propagate nonlinearly, a spherical distance correction dSk cannot be used to allow direct comparison between stations at different distances. Also, sampling frequency can affect dSk values,^{20,21} with higher sampling frequencies better capturing shock rise time, so the data was resampled to 51.2 kHz for consistency between all the channels. The shape of the peak in dSk for April is slightly different than that of September, which seems to correlate with the change in wind speed and direction from upstream to downstream with the plume.

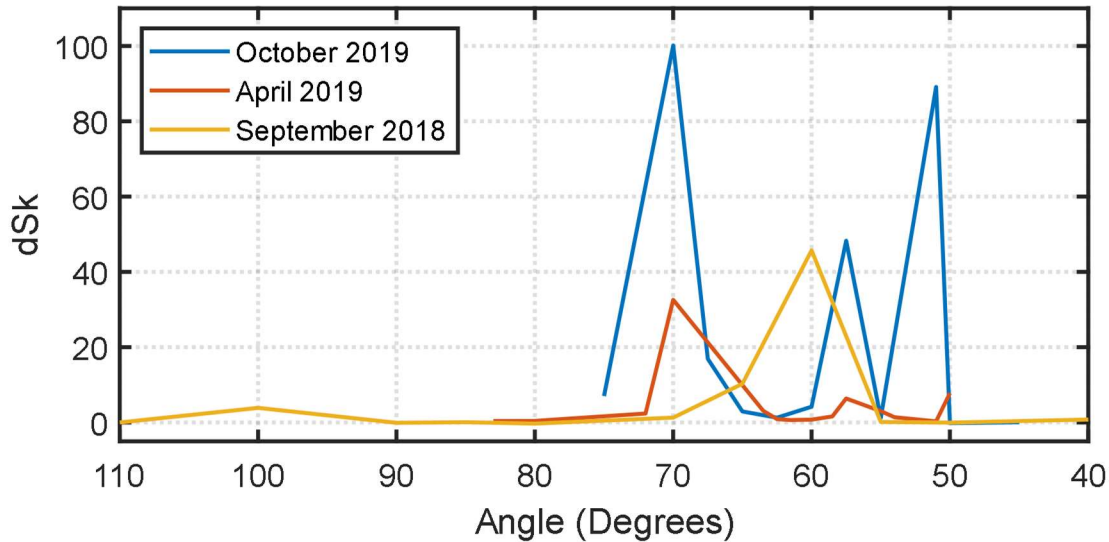


Figure 11. Derivative skewness (dSk) between three firings from the first channel of each station after resampling it to a common frequency of 51.2 kHz.

4. CONCLUSION

Unlike historical measurements and modern mid-field measurements that described a directivity angle of 50-55°, these GEM 63 measurements were able to detect the main radiation lobe of a solid rocket motor in the far field. The September test, with low wind, showed peak directivity at 62° to 63°, which fits prior predictions using the convective Mach wave number. Distance-scaled levels also approximately match those for the same convective Mach number. A pronounced shift can be seen in the dSk directivity between April and September that correlates with the high frequency directivity shift that was noted between the April and September tests. The shift can be attributed to a difference in meteorological conditions, particularly an increase in wind speed and change in wind direction. Future work with these and other GEM 63 measurements will investigate more into the temporal behavior of the firings, particularly in connection with meteorological and terrain effects.

ACKNOWLEDGEMENTS

The author would like Mark C. Anderson, J. Taggart Durrant, Samuel A. Olausson, Francisco J. Irarrazabal, Jacob A. Ward, Mylan R. Cook, Kevin M. Leete, Zachary T. Jones, Aaron B. Vaughn, Jacob R. Smith, and Clark O. Miller for helping collect data, analyze data, or revising the manuscript.

REFERENCES

- ¹K. M. Eldred, *Acoustic loads generated by the propulsion system* (No. NASA SP-8072), (National Aeronautics and Space Administration, 1971).
- ²J. Cole, H. Von Gierke, D. Kyraasis, K. M. Eldred, and A. Humphrey, “Noise radiation from fourteen types of rockets in the 1,000 to 130,000 pounds thrust range.”

³S. McNerny, “Rocket noise-A review,” in (1990) p. 3981. Presented at the 13th Aeroacoustics Conference

⁴S. McNerny, “Characteristics and predictions of far-field rocket noise,” *Noise control engineering journal* **38**, 5–16 (1992).

⁵S. McNerny, “Launch vehicle acoustics. I-Overall levels and spectral characteristics,” *Journal of aircraft* **33**, 511–517 (1996).

⁶J. Haynes, and R. Kenny, “Modifications to the NASA SP-8072 distributed source method II for Ares I lift-off environment predictions,” in (2009) p. 3160. Presented at the 15th AIAA/CEAS Aeroacoustics Conference (30th AIAA Aeroacoustics Conference)

⁷R. Kenny, C. Hobbs, K. Plotkin, and D. Pilkey, “Measurement and characterization of Space Shuttle solid rocket motor plume acoustics,” in (2009) p. 3161. Presented at the 15th AIAA/CEAS Aeroacoustics Conference (30th AIAA Aeroacoustics Conference)

⁸K. L. Gee, R. J. Kenny, T. B. Neilsen, T. W. Jerome, C. M. Hobbs, M. M. James, and 164th Meeting of the Acoustical Society of America, *Spectral and statistical analysis of noise from reusable solid rocket motors*, (2013).

⁹M. M. James, A. R. Salton, K. L. Gee, T. B. Neilsen, S. A. McNerny, and R. J. Kenny, “Modification of directivity curves for a rocket noise model,” in (Acoustical Society of America, 2012) p. 040008. Presented at the Proceedings of Meetings on Acoustics 164ASA

¹⁰K. Gee, J. Giraud, J. Blotter, and S. Sommerfeldt, “Energy-Based Acoustical Measurements of Rocket Noise,” in *15th AIAA/CEAS Aeroacoustics Conference (30th AIAA Aeroacoustics Conference)* (Miami, Florida, American Institute of Aeronautics and Astronautics, 2009). Presented at the 15th AIAA/CEAS Aeroacoustics Conference (30th AIAA Aeroacoustics Conference). doi:[10.2514/6.2009-3165](https://doi.org/10.2514/6.2009-3165)

¹¹K. L. Gee, E. B. Whiting, T. B. Neilsen, M. M. James, and A. R. Salton, “Development of a Near-field Intensity Measurement Capability for Static Rocket Firings,” *AEROSPACE TECHNOLOGY JAPAN* **14**, Po_2_9-Po_2_15 (2016). doi:[10.2322/tastj.14.Po_2_9](https://doi.org/10.2322/tastj.14.Po_2_9)

¹²M. Muhlestein, K. L. Gee, T. B. Neilsen, and D. C. Thomas, “Prediction of nonlinear propagation of noise from a solid rocket motor,” in (Kansas City, Missouri, 2013) pp. 040006–040006. Presented at the 164th Meeting of the Acoustical Society of America. doi:[10.1121/1.4828827](https://doi.org/10.1121/1.4828827)

¹³B. O. Reichman, B. M. Harker, T. B. Neilsen, K. L. Gee, and W.-S. Ohm, “Acoustic measurements in the far field during QM-2 solid rocket motor static firing,” in (Boston, Massachusetts, 2016) p. 045008. Presented at the 173rd Meeting of Acoustical Society of America and 8th Forum Acusticum. doi:[10.1121/2.0000727](https://doi.org/10.1121/2.0000727)

¹⁴*Propulsion Products Catalog* (Catalog), (Northrop Grumman Innovation Systems, 2021). Retrieved from <https://www.northropgrumman.com/wp-content/uploads/NG-Propulsion-Products-Catalog.pdf>

¹⁵K. L. Gee, D. J. Novakovich, L. T. Mathews, M. C. Anderson, and R. D. Rasband, *Development of a Weather-Robust Ground-Based System for Sonic Boom Measurements* (No. NASA/CR-2020-5001870), (National Aeronautics and Space Administration, 2020).

¹⁶B. Greska, A. Krothapalli, W. C. Horne, N. Burnside, “A Near-Field Study of High Temperature Supersonic Jets,” 14th AIAA/CEAS Aeroacoustics Conference (29th AIAA Aeroacoustics Conference), AIAA 2008-3026 (2008).

¹⁷L. T. Mathews, K. L. Gee, and G. W. Hart, “Characterization of Falcon 9 launch vehicle noise from far-field measurements,” *The Journal of the Acoustical Society of America* **150**, 620–633 (2021). doi:[10.1121/10.0005658](https://doi.org/10.1121/10.0005658)

¹⁸H. Oertel, “Measured Velocity Fluctuations Inside the Mixing Layer of a Supersonic Jet,” In *Recent Contributions to Fluid Mechanics*. Springer, Berlin, Heidelberg (1982).

¹⁹K. L. Gee, P. B. Russavage, T. B. Neilsen, S. Hales Swift, and A. B. Vaughn, “Subjective rating of the jet noise crackle percept,” *The Journal of the Acoustical Society of America* **144**, EL40–EL45 (2018). doi:[10.1121/1.5046094](https://doi.org/10.1121/1.5046094)

²⁰K. L. Gee, T. B. Neilsen, A. T. Wall, J. M. Downing, M. M. James, and R. L. McKinley, “Propagation of crackle-containing jet noise from high-performance engines,” *noise cont engng j* **64**, 1–12 (2016). doi:10.3397/1/376354

²¹B. O. Reichman, M. B. Muhlestein, K. L. Gee, T. B. Neilsen, and D. C. Thomas, “Evolution of the derivative skewness for nonlinearly propagating waves,” *The Journal of the Acoustical Society of America* **139**, 1390–1403 (2016). doi:10.1121/1.4944036